Stability of strange stars (SS) derived from a realistic equation of state.

Monika Sinha [1, 2, 3], Jishnu Dey [2, 4 †], Mira Dey [1, 4 †],
Subharthi Ray [5] and Siddhartha Bhowmick, [6]

February 2, 2008

Abstract

A realistic EOS (equation of state) leads to strange stars (ReSS) which are compact in the mass radius plot, close to the Schwarzchild limiting line [1]. Many of the observed stars fit in with this kind of compactness, irrespective of whether they are X-ray pulsars, bursters or soft γ repeaters or even radio pulsars. We point out that a change in the radius of a star can be small or large, when its mass is increasing and this depends on the position of a particular star on the mass radius curve. We carry out a stability analysis against radial oscillations and compare with the EOS of other SS models. We find that the ReSS is stable and an M-R region can be identified to that effect.

(PACS Numbers: 95.30.Cq – 97.10.q – 97.10.Cv – 97.10.Pg – 97.10.Sj – 97.60.Sm – 12.39.x – 51.30.i.)

keywords: compact stars – realistic strange stars – dense matter – elementary particles – equation of state

[1] Dept. of Physics, Presidency College, 86/1 College Street, Kolkata 700 073, India
[2] Azad Physics Centre, Dept. of Physics, Maulana Azad College, 8 Rafi Ahmed Kidwai Road, Kolkata 700 013, India and IUCAA, Pune, India
[3] CSIR-NET fellow, Govt. of India.
[4] Associate, IUCAA, Pune, India
[5] FAPERJ Fellow, Govt. of Brazil, Instituto de Fisica, Université Federal Fluminense, Niteroi, RJ, Brasil
[6] Department of Physics, Barasat Govt. College, Barasat, North 24 Parganas, W. Bengal, India and IUCAA, Pune, India
† permanent address; 1/10 Prince Golam Md. Road, Kolkata 700 026,India;
e-mail : deyjm@giascl01.vsnl.net.in.
* Work supported in part by DST grant no. SP/S2/K21/01, Govt. of India.

1 Introduction

Recently there has been some excitement about the possibility that some compact stars are made from unusual forms of matter [2]. Further, from an analysis of over 1 million seismic data reports sent to the U.S. Geological Survey in the years 1990-93, which were not associated with traditional epicentral sources, Anderson et al. (2002) claim to have found two events that 'have the properties predicted for the passage of a strange quark nugget' through the earth [3]. Approximately 8000 separate seismic stations around the world are included in the database. If confirmed this would be a discovery similar to the detection of gamma ray bursts .

The best observational evidence for the existence of quark stars seems to come from some compact objects like the X-Ray burst sources SAX J1808.4−3658 (the SAX in short) and 4U 1728−34, the X-ray pulsar Her X-1 and the super burster 4U 1820−30. Among these the first is the most stable pulsating X-ray source known to man as of now. This star is claimed to be an ReSS with mass [4] $\sim 1.3\ M_\odot$ and a radius of about 7 km. The mass of 4U 1728−34 is claimed to be less than 1.1 $M_\odot$ in Li et al. [5], which places it much lower in the M-R plot (Fig.1). So it could be still gaining mass and shift to another stable point on the M-R graph. Thus in the model proposed in [1] there is a possible answer to the question posed by Franco [6]: why are the pulsations of SAX not attenuated, as they are in the 4U 1728−34 ?

Fig.1 presents M-R relations for neutron as well as strange stars. The current phenomenology of compact objects could be interpreted to indicate that the mass of a star increases due to accretion so that the radius of a star changes from one point of the stable M-R curve to another. For neutron stars, exemplified by the EOS BBB [1] - the curve on the right in Fig.1 - a smaller mass would imply a larger radius for the star. If the mass of the star increases it should contract. Therefore, expansion due to an increase of mass, subsequent to accretion, is an unstable process for a neutron star. The expected behaviour for SS is directly opposite to that of neutron stars as Fig.1 shows and therefore may support the claim that some compact stars are ReSS.

Coupled to our claim are various other evidences for the existence of ReSS, such as explaining the compact M-R relations of the two candidates given in [1] (namely, the Her X-1 and the 4U 1820−30), as also the possible explanation of two kHz quasiperiodic oscillations in the 4U 1728 - 34 [5].

Recently we found that the matter of an ReSS may have diquarks on the surface which could account for the delayed emission of huge amounts of energy, after a thermonuclear catastrophe. This could be a possible scenario for superbursts [8].

Some of the stars like the SAX J1808.8−3658 or the PSR 1937+21 are fast rotors. ReSS have the possibility of withstanding high rotations which neutron stars or even bag SS cannot sustain. The maximum frequencies for the two EOS of D98 are 2.6 and 2.8 kHz respectively when they are on the mass shed limit (supramassive model) and 1.8 kHz and 2 kHz when they are in the normal evolutionary sequence as shown in Gondek-Rosińska et al. [9]. In the present paper we further show that the ReSS are not only stable under fast rotation but also against

[1] this is one of the set calculated by Baldo, Bombaci and Burgeo [7] using a realistic nuclear equation of state.

radial oscillations.

The strange matter hypothesis has been used to postulate a scenario whereby a neutron star collapses to a quark star, simultaneously with a gamma ray burst - the so called phenomenon of a quark nova [10].

In the cosmic separation of phase scenario of Witten [11] SS are created along with baryons in a hot environment during the expansion of the early universe. The problem was investigated for ReSS [12] and it was found that they are formed at a temperature $T \sim 70\ MeV$. Since it is self-sustaining, the system expands as the Universe cools, the ReSS expands like the Universe itself with cooling [12]. The calculation also suggests that the shift in entropy due the change from normal to strange matter is not very large, indicating that the phase transition is relatively smooth.

We note that in a series of early papers van Paradijs ([13]) had noted that (i) the X-rays for bursters originate from stars with radii around 7 kms, assuming a canonical mass of 1.4 $M_{\odot}$ for them and (ii) if one assumes a lower mass the estimated radii also becomes lower, which fits the M-R relation for the ReSS (Fig. 1)

Because of the extremely strong electric field stretching outside the stellar surface within $\sim 10^{-10}$ cm [14] Usov [15] suggested that at a finite surface temperature ($5 \times 10^8\ K$) of an SS one expects to have the creation of e^+e^- pairs on its surface. Such an effect could be an additional observational signature of SS with nearly bare quark surfaces. The strange matter equilibrium will not allow the pair production to quench, contrary to the comment in [16] as pointed out in [17]. Usov claimed that the chemical potential of the electrons at the surface is large compared to their mass, being around 20 MeV and the mean velocity of the electrons is very high, so that the electric field will be restored very quickly. In our calculations we specifically find this to be ∼29 MeV, thus strongly supporting the conclusions of Usov.

Usov has further claimed that from the nature of the two step process, viz. e^+e^- pair production and subsequent γ emission, the soft γ repeaters are indeed very young SS [18] and their genesis may be due to the impact of comet like objects with these stars [19].

We must also add that radio pulsars may be SS as was suggested recently by Xu et al [20] for the PSR 0943+10 and all other drifting pulsars. Further, Kapoor and Shukre [21] used a remarkably precise observational relation for pulsar core component widths of radio pulsars to get stringent limits on pulsar radii, strongly indicating that some pulsars are strange stars. This is achieved by including general relativistic effects due to the pulsar mass on the size of the emission region needed to explain the observed pulse widths. A recent paper supporting their ideas is Xu, Xu and Wu [22] for PSR 1937+21,the fastest known radio pulsar.

The calculations for cold ReSS by Dey et al. [1] enables us to draw conclusions about chiral symmetry restoration (CSR) in QCD when the EOS is used to get ReSS fitting definite M-R relations [1, 4, 5]. The empirical M-R relations were derived from astrophysical observations like luminosity variation and some properties of quasiperiodic oscillations from compact stars. The density dependence of the strong coupling constant can be deduced from the CSR described above [23].

Recently Glendenning [24] has argued that the SAX could be explained as a neutron star

rather than a bare SS, not with any of the existing known EOS, but with a hypothetical one, satisfying however, the well-accepted restrictions based on general physical principles and having a core density about 26 ρ_0. Of course, such high density cores imply hybrid strange stars, subject to Glendenning's assumption that such stars can exist with matching EOS for two phases. There is the further constraint that if the most compact hybrid star has a given mass, all lighter stars must be larger. It was found in Li et al. [5] that the star 4U 1728−34 may have a mass less than that of the SAX and yet have a smaller radius. Another serious difference is that the EOS of D98, using the formalism of large N_c approximation, indeed shows a bound state in the sense of having a minimum at about 4.8 n_0, whereas in Glendenning [24] one of the assumptions is that strange matter has no bound state.

2 ReSS model - the EOS

The model solves the relativistic mean field equation with a realistic qq interaction, the quark masses decreasing with density and restoring to their current mass values at high enough density. Moreover, the bare, confining qq interaction is expected to get screened in the medium. The inverse Debye screening length (D^{-1}) is an increasing function of density. With these two conditions, namely the tendencies towards deconfinement and chiral symmetry restoration with density, we set out to obtain the required EOS for beta-equilibrated, charge neutral strange quark matter (SQM) containing uds quarks.

The plausibility condition for SQM to be preferred to ordinary matter is,

$$E_{ud}/A \; > \; E_{Fe^{56}}/A \; > \; E_{uds}/A \tag{1}$$

In Fig.2 we have shown that the energy per baryon for our equation of state (EOS1 of [1]) has a minimum at E/A = 888.8 MeV compared to 930.4 of Fe^{56}. The pressure at this point is zero and this marks the surface of the star as can be seen when the well known TOV equation is solved. The curve clearly shows that the system can fluctuate about this minimum - so that the zero pressure point can vary. The EOS is parameterized to a linear form in [9] as

$$p = a(\epsilon - \epsilon_0), \tag{2}$$

where a and ϵ_0 are two parameters, $a = 0.463$ and $\epsilon_0 = 1.15 \times 10^{15}$ $gm\ cm^{-3}$.
For EOS3 they are $a = 0.455$, $\epsilon_0 = 1.33 \times 10^{15}$ $gm\ cm^{-3}$. Sharma et al [25] showed that the model possesses scaling properties similar to the bag model.

The bag model EOS, which satisfies the plausibility condition Eq.(1), must have a bag constant which cannot be higher than 75 MeV/fm^3 when the strange quark mass is taken to be 150 MeV. We have plotted this EOS as a dashed curve in Fig.2. The minimum in E/A is seen to occur at a low density, about $\sim 2n_0$ where n_0 is the normal nuclear matter density of $0.17/fm^3$. This kind of density may have been already reached in present day heavy ion collision experiments and yet no clear signature of stable strange matter has been observed. This problem does not occur with ReSS where the surface density is about $\sim 5\ n_0$. In addition

to this, the bag does not fit the M-R data for the strange star candidates as has been repeatedly stated before [1, 4, 5]. The minimum of energy of the bag model (dashed curve) is 921 MeV. The gain in energy in strange matter, using the bag model, is only a few MeV over Fe^{56}, of the order of thermonuclear energy release. For the realistic EOS it is much larger ~ 40 MeV.

The unusually hard X-ray burster GRO J1744−28 [26] or the soft γ repeaters [27] require the strange star models, since these stars require an energy release which is large compared to thermonuclear energies. With the bag model that would fit the requirement Eq.(1), it is difficult to explain the hard X-ray bursters or soft γ repeaters since the energy gain over Fe^{56} is only ~ 3 MeV.

3 Mass - Radius

Quasiperiodic oscillations in the 4U 1728−34, led to the idea that it is an ReSS [5] with a mass $1.1M_{\odot}$. The star is 4.3 kpc away.

We elaborate on the point mentioned above, namely that if an SS gains mass due to accretion its radius might not necessarily change. We demonstrate this in Fig.3 by the horizontal tangent line drawn on the ReSS M-R relation. It is possible that the X-rays or γ rays emitted by a compact object is due to the conversion of the accreting normal matter to strange matter [28]. The energy gain by a baryon on conversion is nearly ~ 40 MeV or so, making it a very favourable event. Thus a star of small mass may become heavier with a consequent increase of the radius. However, when it reaches the horizontal line $\frac{dR}{dM}$ is zero and its radius does not increase for some time. We have fitted the M-R curve to a polynomial,

$$R(M) \;=\; \sum_{i=1}^{7} \; a_i \; \left(\frac{M}{M_{\odot}}\right)^i \tag{3}$$

The parameters a_i are given in Table 1 for the convenience of possible users. The parameters obtained from the two EOS are given in Table 2.

It is found that some X-ray bursters like the 4U 1728−34 do not show any radial expansion whereas others like the KS 1731−260 are usually observed only in bursts that exhibit photospheric expansion [29]. We conjecture that the persistently bright X-ray transient KS 1731−260 was a low mass star gaining mass and thus a radius expansion was allowed by the TOV stability criterion. After 11.5 years of activity this source was detected in January 2001 with *Chandra* in quiescence with a luminosity that is comparable to other normal X-ray emitting compact stars [30]. This could also be explained if the star, in these decade of expansion, has reached the same stage as the 4U 1728−34.

4 Radial oscillations of a relativistic star

Thirty five years ago Chandrasekhar [31] investigated these radial modes. They give information about the stability of a stellar model. Recently such studies have been carried out for many

existing neutron star EOS [32]. Sharma et al [25] made a stability analysis of Eqn. (2) and found that the EOS is stable against radial oscillations. However, a more detailed analysis is needed to restrict the M-R relation. For completeness an outline of the scheme is given below.

The spherically symmetric metric is given by the line element

$$ds^2 = -e^{2\nu}dt^2 + e^{2\mu}dr^2 + r^2(d\theta^2 + \sin^2\theta d\phi^2). \tag{4}$$

Together with the energy-momentum tensor for a perfect fluid, Einstein's field equations yield the TOV equation which can be solved if we have an EOS, $p(n_B)$ and $\epsilon(n_B)$. Given the central density ϵ_c, we can arrive at an $M-R$ curve by solving the TOV. Without disturbing the spherical symmetry of the background we define $\delta r(r,t)$, a time dependent radial displacement of a fluid element located at the position r in the unperturbed model which assumes a harmonic time dependence, as

$$\delta r(r,t) = u_n(r)e^{i\omega_n t}. \tag{5}$$

The dynamical equation governing the stellar pulsation in its nth normal mode ($n = 0$, is the fundamental mode) has the Sturm-Liouville's form (for details, see [33])

$$P(r)\frac{d^2u_n(r)}{dr^2} + \frac{dP}{dr}\frac{du_n}{dr} + \left[Q(r) + \omega_n^2 W(r)\right]u_n(r) = 0, \tag{6}$$

where $u_n(r)$ and ω_n are the amplitude and frequency of the nth normal mode, respectively. The functions $P(r)$, $Q(r)$ and $W(r)$ are expressed in terms of the equilibrium configuration of the star and are given by

$$P(r) = \frac{\Gamma p}{r^2}e^{\mu+3\nu} \tag{7}$$

$$Q(r) = e^{\mu+3\nu}\left[\frac{(p')^2}{r^2(\epsilon+p)} - \frac{4p'}{r^3} - \frac{8\pi}{r^2}(\epsilon+p)\ p\ e^{2\mu}\right] \tag{8}$$

$$W = \frac{(\epsilon+p)}{r^2}\ e^{3\mu+\nu}, \tag{9}$$

where the varying adiabatic index Γ is given by

$$\Gamma = \frac{(\epsilon+p)}{p}\frac{dp}{d\epsilon}, \tag{10}$$

ϵ and p being the energy density and pressure of the unperturbed model, respectively. Eigenfrequencies can be obtained with the boundary conditions,

1. at the centre $r = 0$, $\delta r = 0$ and
2. at the surface $\delta p = 0$ leading to $\Gamma\ p\ u(r)' = 0$,

Since ω is real for $\omega^2 > 0$, the solution is oscillatory. However for $\omega^2 < 0$, the angular frequency ω is imaginary, which corresponds to an exponentially growing solution. This means that for negative values of ω^2 the radial oscillations are unstable. For a compact star the fundamental mode ω_0 becomes imaginary at some central density ϵ_c less than the critical density $\epsilon_{critical}$ for which the total mass M is a maximum. At $\epsilon_c = \epsilon_c^0$, ω_0 vanishes. All higher modes are zero at even higher central densities. Therefore, the star is unstable for central densities greater than ϵ_c^0. To illustrate, we plot the eigenfrequencies ω_n against ϵ_c, the central density in Fig. 5. The fundamental frequency ω_0 does vanish at some ϵ_c^0 while the higher modes remain nonzero.

Numerical values of masses, radii, central densities and the corresponding eigenfrequencies ω_0, ω_1 and ω_2 are given in Tables 3 and 4 for our EOS1 (SS1[1]) and EOS3(SS2[1]) respectively. The corresponding linear fits described by Eqn.(2) for SS1 and SS2 are given in Table 5 and 6. Tables 7 and 8 are for the bag model EOS with different parameters.

5 Discussions and summary

In summary, evidence for the existence of strange stars have been accumulating. In the present paper we review possible candidates and suggest that the properties peculiar to some of the compact stars can be explained if they are SS. In particular we point out that mass accumulation due to accretion does not lead to an increase in the radius for stars like the 4U 1728−34, claimed to be low mass SS from accretion data [5]. If some compact objects are proven to be ReSS then parameterizations of QCD chiral symmetry restoration at high densities for quarks, the smallest particles known, can be achieved with the help of data from some of the heaviest objects in the Universe.

ReSS are stable against radial oscillations close to the maximum attainable mass. For example, the EOS of SS1 sustains gravitationally, $M_{max} \sim 1.4 M_\odot$, R=7 km with a central number density $n_c \sim 16 n_0$. However, the fundamental frequency of radial oscillations becomes zero at around n_c 9.5 $\sim n_0$, destabilizing the star after M=1.36 $M_\odot$ with R= 7.24 km (Table 3). It is still on the $\frac{dM}{dR} > 0$ region. Thus the maximum mass star which is stable against radial oscillations has a number density $\sim 9.5 n_0$ at the centre and $\sim 4.7 n_0$ at the surface. Macroscopically, upto this density small vibrations may be sustained.

A corresponding linear fit has the stable values M=1.34 $M_\odot$ and R=7.35 km(Table 5). Radial oscillation is rather sensitive and the fit is better than 3%(Tables 3 and 5). The same pattern is seen for SS2 and the corresponding linear fit (Tables 4 and 6). Thus we see that almost all of the M-R region is stable.

There has been a recent controversy about the star RXJ1856.−3754 − whether it can be inferred to be a strange star [2, 34]. Analysis of the observational data of this "no pulsar", 120 pc away, cool star is not conclusive. As noted by [35] the stable portion of the $M - R$ region shown in Fig. 4 can accommodate this star very easily. This could be a possible candidate of our SS model provided its mass and radius are established beyond controversy.

Acknowledgements: The sad demise of our collaborator Dr. Ranjan Ray was painful for us. We dedicate this paper to his memory. MD and MS thank the RRI for hospitality and JD, MS and SB thank the IUCAA.

References

[1] M. Dey, I. Bombaci, J. Dey, S. Ray & B. C. Samanta, Phys. Lett. **B438** 123 (1998) ; Addendum B447 (1999) 352; Erratum B467 (1999) 303; Indian J. Phys. 73B (1999) 377.

[2] J. J. Drake et al, Is RXJ1856.5−3754 a Quark Star?, astro-ph/0204159 v1, Ap. J. **572** (2002) 996.

[3] D. P. Anderson, E. T. Herrin, V. L. Teplitz and I. M. Tibulaec, 'Two Seismic Events with the Properties for the Passage of Strange Quark Matter Through the Earth', astro-ph/0205089.

[4] X. Li, I. Bombaci, M. Dey, J. Dey & E. P. J. van den Heuvel, Phys. Rev. Lett. **83** 3776 (1999).

[5] X. Li, S. Ray, J. Dey, M. Dey & I. Bombaci, Ap. J. **527** L51 (1999).

[6] L. M. Franco, The Effect of Mass Accretion Rate on the Burst Oscillations in 4U 1728-34. astro-ph/0009189, Ap. J. **554** 340 (2001).

[7] M. Baldo, I. Bombaci & G. F. Burgio, Astron. & Astrophys. **328** 274 (1997).

[8] M. Sinha, M. Dey, S. Ray and J. Dey, Superbursts and long bursts as surface phenomenon of compact objects (to be published).

[9] D. Gondek-Rosińska , T. Bulik , L. Zdunik , E. Gourgoulhon , S. Ray , J. Dey & M. Dey, Astron. & Astrophys. **363** 1005 (2000).

[10] R. Ouyed, J. Dey and M. Dey, astro-ph/0105109v3, Astron. & Astrophys. (in press).

[11] E. Witten, Phys. Rev. D **30** 272 (1984).

[12] S. Ray, J. Dey , M. Dey , K. Ray & B. C. Samanta, Astron. & Astrophys. **364** L89 (2000).

[13] J. V. Paradijs, Nature **274** 650 (1978); J. V. Paradijs, Ap. J. **234** 609 (1979); J. V. Paradijs, Astron. & Astrophys. **101** 174 (1981).

[14] C. Alcock, Nucl. Phys. B. (Proc. Suppl.) **24** 93 (1991).

[15] V. V. Usov, Ap. J. 481 (1997) L107. ; V. V. Usov, Phys. Rev. Lett. **80** 230 (1998).

[16] A. Mitra, Phys. Rev. Lett., **81** 4774 (1998).

[17] V. V. Usov, Phys. Rev. Lett. **81** 4775 (1998).

[18] V. V. Usov, Ap. J. **550** L179 (2001).

[19] V. V. Usov, Phys. Rev. Lett.**87** 021101 (2001).

[20] R-X. Xu, G. J. Qiao & B. Zhang, Ap. J. **522** L109 (1999).

[21] R. C. Kapoor and C. S. Shukre, "Are radio pulsars strange stars?" astro-ph/0011386, Astron. and Astrophys. **375** 405 (2001).

[22] R-X. Xu, X-B. Xu & X-J. Wu, Chin. Phys. Lett. **18** 837 (2001).

[23] S. Ray, J. Dey & M. Dey Mod. Phys. Lett. A **15** 1301 (2000).

[24] N. Glendenning, Phys. Rev. Lett. **85** 1150 (2000).

[25] R. Sharma, S. Mukherjee, Mira Dey and Jishnu Dey, Mod. Phys. Lett. A **17** 827 (2002).

[26] K. S. Cheng, Z, G. Dai, D. M. Wai & T. Lu Science, **280** 407 (1998).

[27] K. S. Cheng & Z. G. Dai, Phys. Rev. Lett. **80** 18 (1998) .

[28] I. Bombaci and B. Datta, Ap. J. **530** L69 (2000).

[29] M. P. Muno, D. Chakrabarty, D. K. Galloway and P. Savov, Ap. J. **553** L157 (2001).

[30] R. Wijnands, J. M. Miller, C. Markwardt, W. H. G. Lewin and M. van der Klis, 'A *Chandra* observation of the long-duration X-ray transient KS 1731−260 in quiescence : too cold a neutron star?', astro-ph/0107380, submitted to Ap. J. Letters.

[31] S. Chandrasekhar, Phys. Rev. Lett. **12** 114 (1964) ; Ap. J, **217** 417 (1964) .

[32] K.D. Kokkotus and J. Ruoff, A & A A, **366** 565 (2001) ; V.K. Gupta, Vinita Tuli and Ashoke Goyal, astro-ph/0202016.

[33] C.W. Misner, K.S. Throne & J. A. Wheeler, *Gravitation*, W. H. Free man & Co. New York (1973).

[34] Jose A. Pons et al , Ap. J., **564** 981 (2002).

[35] A.R. Prasanna and Subharthi Ray, astro-ph/0205343.

Table 1: Parameters for the M-R curve in Fig.3

i	1	2	3	4	5	6	7
a_i	-343.7	2134	-5265	6805	-4884	1848	-288.4

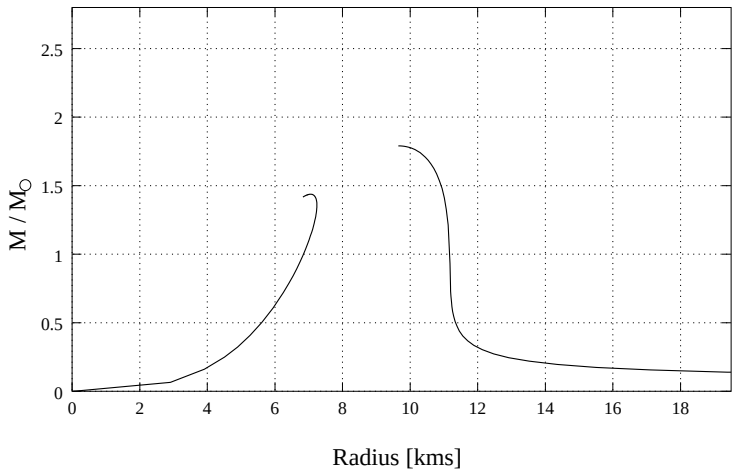

Figure 1: The mass and radius of stable stars with the strange star EOS (left curve) and neutron star EOS (right curve), which are solutions of the Tolman-Oppenheimer-Volkoff (TOV) equations of general relativity. Note that self sustained strange star systems can have small masses and radii, whereas neutron stars have large radii for smaller masses since they are bound by gravitation.

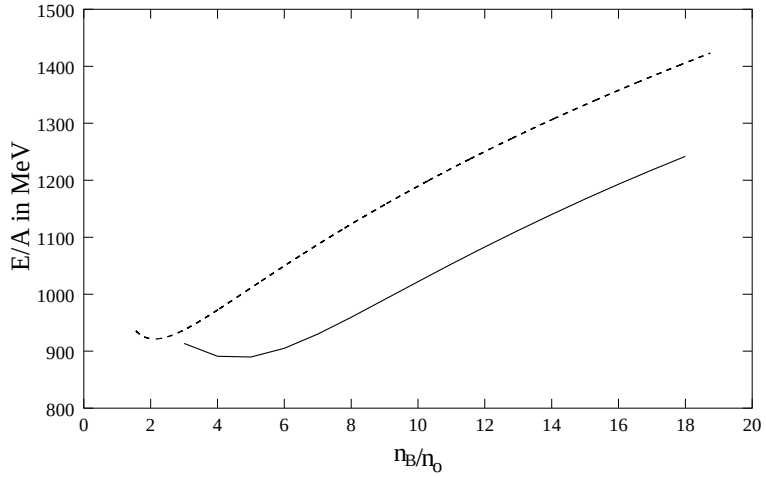

Figure 2: The eos1 in d98 shows that there is a stable point in the strange matter which has energy per baryon less than that of Fe^{56} by more than 40 MeV (lower curve) . The dashed curve shows a bag model EOS with B=72 MeV/fm^3 with non-interacting massless u,d quarks and m_s = 150 MeV. (upper curve)

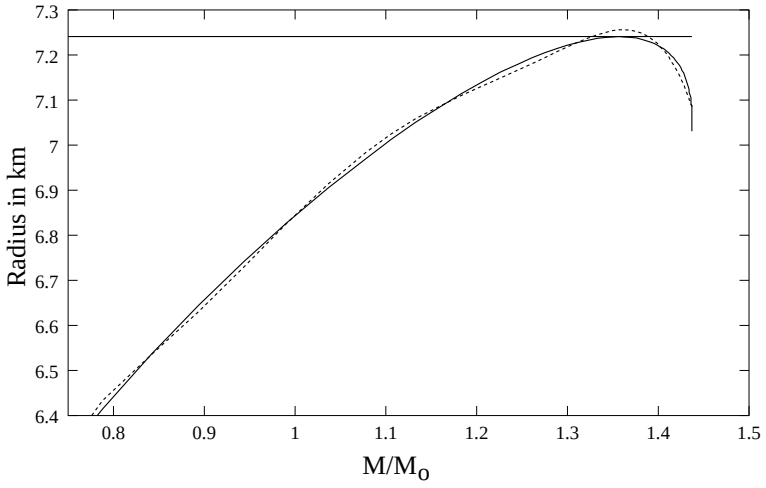

Figure 3: The radius of a star plotted as a function of its mass for EOS1. The horizontal line is the tangent drawn at the maximum radius. The fitted polynomial is shown by a dashed curve.

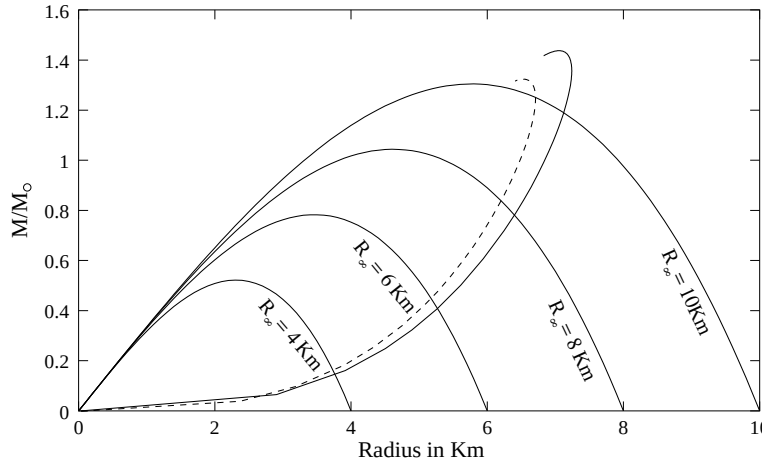

Figure 4: Allowed M-R region with two EOSs, solid curve for EOS1 and dashed curve for EOS3.

Table 2: Parameters from the two EOS

EOS	$M_G/M_\odot$	R (km)	n_c/n_o	ϵ_c $(10^{14}g/c.c.)$	n_s/n_o
SS1	1.437	7.055	13.669	46.85	4.586
SS2	1.325	6.5187	15.537	55.17	5.048

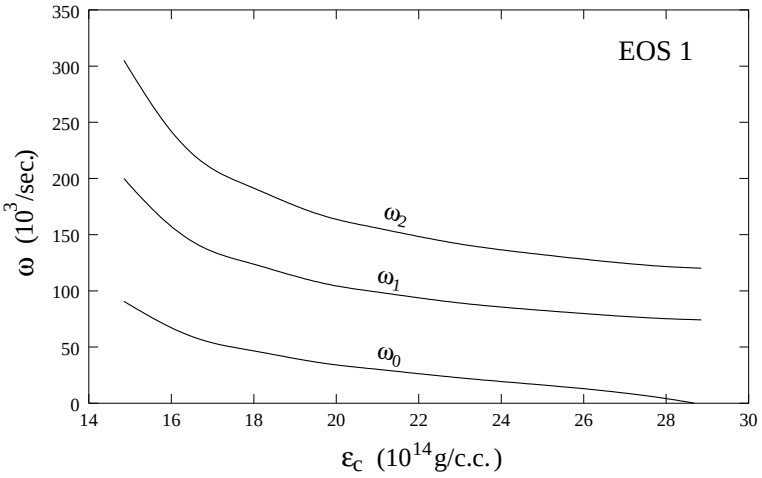

Figure 5: Angular frequency of three different modes against central density for SS1.

Table 3: Data for EOS1 (SS1)

ρ_c 10^{14} g/c.c.	n_c/n_0	$M/M_\odot$	R km	ω_0 10^3 /sec.	ω_1 10^3 /sec.	ω_2 10^3 /sec.
14.85	5.462	0.407	5.262	90.661	199.957	305.202
15.85	5.798	0.502	5.611	79.884	179.851	275.679
16.85	6.122	0.787	5.940	69.870	162.018	249.011
17.85	6.429	0.893	6.643	47.528	125.267	193.718
18.85	6.735	0.991	6.828	40.784	114.643	178.073
19.85	7.036	1.077	6.970	34.751	105.455	165.102
20.85	7.321	1.133	7.050	30.694	99.662	156.925
21.85	7.605	1.182	7.113	26.848	94.509	149.451
22.85	7.886	1.226	7.161	23.077	89.825	142.620
23.85	8.159	1.261	7.193	19.749	86.070	137.200
24.85	8.427	1.288	7.214	16.693	83.005	132.804
25.85	8.692	1.312	7.228	13.435	80.192	128.753
26.85	8.955	1.333	7.236	9.648	77.588	135.005
27.85	9.212	1.349	7.240	4.943	75.483	122.982
28.85	9.466	1.363	7.240	5.899	73.592	119.295
30.85	9.969	1.381	7.235	–	70.168	114.425
35.85	11.176	1.417	7.194	–	64.144	105.945
40.85	12.333	1.433	7.130	–	59.935	100.169
46.85	13.669	1.437	7.055	–	56.349	95.361

Table 4: Data for EOS3 (SS2)

$\rho_c \times 10^{14}$ g/c.c.	n_c/n_0	$M/M_\odot$	R km	$\omega_0 \times 10^3$ /sec.	$\omega_1 \times 10^3$ /sec.	$\omega_2 \times 10^3$ /sec.
17.17	6.067	0.423	5.070	86.879	195.416	299.090
18.17	6.382	0.539	5.460	74.016	172.966	264.894
19.17	6.695	0.659	5.794	63.013	153.699	236.761
20.17	7.006	0.781	6.078	53.079	136.745	212.463
21.17	7.298	0.855	6.227	47.332	127.643	199.063
22.17	7.588	0.923	6.351	42.074	119.663	186.932
23.17	7.876	0.986	6.453	37.131	112.402	176.070
24.17	8.156	1.036	6.524	33.069	106.694	167.790
25.17	8.428	1.075	6.575	29.646	102.152	161.274
26.17	8.699	1.110	6.615	26.321	98.030	155.270
27.17	8.967	1.142	6.647	22.992	94.193	149.689
28.17	9.227	1.167	6.667	20.163	91.206	145.298
29.17	9.485	1.188	6.682	17.335	88.518	141.539
30.17	9.741	1.207	6.693	14.307	86.006	137.932
31.17	9.994	1.224	6.691	10.827	83.642	134.554
32.17	10.242	1.237	6.702	6.982	81.741	131.825
33.17	10.488	1.249	6.703	3.351	79.959	129.293
35.17	10.974	1.270	6.698	–	76.694	124.666
40.17	12.148	1.301	6.650	–	70.680	116.215
45.17	13.278	1.316	6.622	–	66.380	110.292
50.17	14.371	1.323	6.573	–	63.141	105.918
55.17	15.537	1.325	6.518	–	60.616	102.546

Table 5: Data for SS1 from fitted EOS1

$\rho_c \times 10^{14}$ g/c.c.	n_c/n_0	$M/M_\odot$	R km	$\omega_0 \times 10^3$ /sec.	$\omega_1 \times 10^3$ /sec.	$\omega_2 \times 10^3$ /sec.
14.85	5.436	0.635	6.188	59.977	144.353	222.426
15.85	5.763	0.770	6.544	49.791	127.744	196.858
16.85	6.081	0.879	6.787	42.407	114.994	179.262
17.85	6.392	0.968	6.957	36.671	106.205	166.319
18.85	6.697	1.041	7.079	31.962	99.289	156.335
19.85	6.994	1.101	7.167	27.938	93.826	148.390
20.85	7.287	1.152	7.230	24.376	89.333	141.887
21.85	7.573	1.194	7.276	21.115	85.580	136.461
22.85	7.855	1.229	7.307	18.025	82.380	131.844
23.85	8.132	1.260	7.329	14.976	79.615	127.894
24.85	8.405	1.286	7.342	11.780	77.195	124.449
25.85	8.674	1.308	7.350	8.036	75.052	121.420
26.85	8.939	1.327	7.352	1.034	73.175	118.733
27.85	9.201	1.343	7.350	7.078	71.465	116.329
30.85	9.840	1.380	7.329	–	67.274	110.448
35.85	11.184	1.415	7.265	–	62.242	103.549
40.85	12.343	1.431	7.187	–	58.683	98.749
46.85	13.671	1.436	7.091	–	55.523	94.636

Table 6: Data for SS2 from fitted EOS3

$\rho_c \times 10^{14}$ g/c.c.	n_c/n_0	$M/M_\odot$	R km	$\omega_0 \times 10^3$ /sec.	$\omega_1 \times 10^3$ /sec.	$\omega_2 \times 10^3$ /sec.
17.17	6.036	0.579	5.718	64.793	155.655	239.799
18.17	6.351	0.688	6.013	55.081	139.070	215.380
19.17	6.659	0.779	6.224	47.803	127.136	197.858
20.17	6.961	0.855	6.378	42.037	118.072	184.600
21.17	7.257	0.919	6.494	37.269	110.906	174.149
22.17	7.547	0.973	6.581	33.177	105.095	165.697
23.17	7.833	1.019	6.646	29.567	100.382	158.683
24.17	8.114	1.059	6.696	26.300	96.185	152.771
25.17	8.390	1.093	6.733	23.270	92.680	147.719
26.17	8.663	1.122	6.761	20.392	89.632	143.331
27.17	8.931	1.148	6.781	17.584	86.947	139.496
28.17	9.196	1.170	6.795	14.749	84.584	136.101
29.17	9.458	1.190	6.804	11.724	82.467	133.077
30.17	9.716	1.207	6.809	8.129	80.545	130.365
31.17	9.971	1.222	6.811	1.818	78.823	127.914
32.17	10.224	1.235	6.809	6.940	77.243	125.684
35.17	10.964	1.266	6.795	–	73.257	120.094
40.17	12.140	1.298	6.747	–	68.293	113.270
45.17	13.286	1.314	6.688	–	64.668	108.365
50.17	14.379	1.322	6.624	–	61.862	104.656
55.17	15.332	1.324	6.561	–	59.601	101.747

Table 7: Data for bag model with B=60 & ms=150

$\rho_c \times 10^{14}$ g/c.c.	n_c/n_0	$M/M_\odot$	R km	$\omega_0 \times 10^3$ /sec.	$\omega_1 \times 10^3$ /sec.	$\omega_2 \times 10^3$ /sec.
6.20	2.421	0.691	8.549	38.964	92.549	142.426
7.20	2.778	1.019	9.544	27.409	73.557	114.644
8.20	3.122	1.240	10.021	20.733	63.870	100.636
9.20	3.454	1.393	10.263	15.915	57.854	92.024
10.20	3.776	1.501	10.393	11.910	53.693	86.161
11.20	4.089	1.581	10.452	7.900	50.628	81.883
12.20	4.396	1.639	10.469	2.159	48.272	78.626
13.20	4.695	1.683	10.462	6.156	46.395	76.048
15.20	5.277	1.741	10.405	–	43.526	72.203
17.20	5.839	1.775	10.321	–	41.429	69.514
23.70	7.560	1.805	10.012	–	37.316	64.404

Table 8: Data for bag model with B=75 & ms=150

$\rho_c \times 10^{14}$ g/c.c.	n_c/n_0	$M/M_\odot$	R km	$\omega_0 \times 10^3$ /sec.	$\omega_1 \times 10^3$ /sec.	$\omega_2 \times 10^3$ /sec.
9.83	3.573	1.072	8.923	24.809	73.494	115.482
10.83	3.892	1.198	9.148	20.030	67.175	106.403
11.83	4.203	1.293	9.281	16.097	62.623	99.944
12.83	4.506	1.366	9.356	12.565	59.194	95.089
13.83	4.804	1.422	9.396	9.063	56.480	91.314
14.83	5.095	1.467	9.412	4.502	54.280	88.272
15.83	5.318	1.502	9.411	4.887	52.470	85.769
20.83	6.748	1.594	9.294	–	46.505	77.834
25.83	8.031	1.622	9.123	–	43.109	73.610
28.83	8.769	1.626	9.020	–	41.638	71.868